journal

J. Am. Ceram. Soc., 85 [10] 2462–68 (2002)

Effect of pH of Medium on Hydrothermal Synthesis of Nanocrystalline Cerium(IV) Oxide Powders

Nan-Chun Wu, Er-Wei Shi, Yan-Qing Zheng, and Wen-Jun Li

Shanghai Institute of Ceramics, Chinese Academy of Sciences, Shanghai 201800, People's Republic of China

Well-crystallized cerium(IV) oxide (CeO_2) powders with nanosizes without agglomeration have been synthesized by a hydrothermal method in an acidic medium by using cerium hydroxide gel as a precursor. The relationship between the grain size, the morphology of the CeO_2 crystallites, and the reaction conditions such as temperature, time, and acidity of the medium was studied. The experiments showed that with increasing reaction temperature and time, the CeO_2 crystallites grew larger. The crystallites synthesized in an acidic hydrothermal medium were larger and had a more regular morphology than the ones synthesized in a neutral or alkaline medium when the reaction temperature and time were fixed. The CeO_2 crystallites synthesized in an acidic medium were monodispersed; however, there was vigorous agglomeration among the grains synthesized in a neutral or alkaline medium. It was demonstrated that the hydrothermal treatment was an Ostwald ripening process and the acidity (pH) of the used hydrothermal medium played a key role in the dissolution of smaller grains. It is proposed that the dissolution process can control the kinetics of the growth of larger grains.

I. Introduction

CERIA (CeO_2) is currently being used not only as an oxygen ion conductor in solid oxide fuel cells (SOFCs)[1,2] and oxygen monitors[3] but also as catalytic supports[4–6] of automotive exhaust systems because of its high oxygen ion conductivity. It has been considered that the properties of the materials may be greatly improved if ultrafine powders are used as a raw material. Therefore, preparation of ultrafine CeO_2 powders without agglomeration has been intensively investigated.

Several techniques that include hydrothermal synthesis,[7–11] urea-based homogeneous precipitation,[12,13] hexamethylenetetramine-based homogeneous precipitation,[14] coprecipitation,[15] decomposition of oxalate precursors,[16] and mechanical mixing[17] have been developed for the production of ceria or cation-doped ceria particles. As a low-temperature and wet-chemical technique, hydrothermal methods offer an exciting possibility for the synthesis of high-purity, homogeneous, and ultrafine powders. Zhou and Rahaman[9] reported the sintering behaviors of CeO_2 and Y_2O_3-doped CeO_2 powders synthesized by a hydrothermal method from $Ce(NO_3)_3$ solution and ammonium hydroxide solution. Tani and co-workers[10] studied the effect of used mineralizers on hydrothermal synthesis of CeO_2 powders. Hirano and his co-workers[11] showed controlled crystallization of CeO_2 particles during hydrothermal synthesis from Ce(IV) salts. It has been found that the agglomeration of hydrothermal CeO_2 powders is vigorous though the particle size is very fine.

Cerium hydroxide formed from Ce(IV) or Ce(III) salt solutions can be used as a precursor for hydrothermal synthesis of CeO_2 powders. A series of precursor reactions such as polymerizing, dehydrating, and dehydrogenating will occur under hydrothermal conditions and play a key role in the formation of CeO_2 crystallites. Otherwise, acidity of the hydrothermal medium has direct influence on the structure and reaction of cerium hydroxide. Therefore, it is very important to understand the formation mechanism of CeO_2 crystallites in the hydrothermal reaction mediums with different acidities. In this article, the effect of the pH of the reaction medium on the crystallization of CeO_2 grains under hydrothermal conditions when cerium hydroxide is used as a precursor is reported, as well as the synthesis of nanocrystalline CeO_2 powders without agglomeration.

II. Experimental Procedure

(1) Hydrothermal Synthesis of CeO_2 Powders

The starting materials were cerium(IV) sulfate tetrahydrate ($Ce(SO_4)_2 \cdot 4H_2O$) and sodium hydroxide (NaOH) (AR grade purity). The appropriate amounts of $Ce(SO_4)_2 \cdot 4H_2O$ and NaOH were respectively dissolved in distilled water to form 0.1*M* $Ce(SO_4)_2$ and 0.4*M* NaOH solutions. When the $Ce(SO_4)_2$ solution was added to the NaOH solution, precipitates (gel) were formed immediately. After being filtered and washed by distilled water, the precipitates (gel) as a precursor were put into an autoclave with a reaction chamber of 40 cm^3. Three quarters of the volume of the chamber was filled with solutions. The acidity of the reaction medium was adjusted by adding HCl or NaOH solutions. The hydrothermal experiments were performed in the media with pH values of 2, 7, and 12. The hydrothermal syntheses were carried out in a temperature range from room temperature to 245°C and the time ranged from 18 to 120 h, corresponding to a pressure range from 1 to 60 bar. After the hydrothermal reaction, the products (powders) were filtered, washed with distilled water several times, and air-dried at 110°C for 7 h.

(2) Characterization of the Powders

The phase identification of the products was carried out by X-ray powder diffraction (XRD; Rigaku RAX-10). Grain sizes were estimated by line-broadening analysis according to the formula $D = 0.9\lambda/(\beta \cos \theta)$, where D is the grain size, λ is the wavelength of X-rays, θ is the diffraction angle, and β is the half-width of the diffraction peaks. The morphology of the crystallites was observed by transmission electron microscopy (TEM, JEOL JEM-2010). The chemical composition of the products was determined by X-ray fluorescence spectroscopy (XRFS, Philips TW-2404) and inductively coupled plasma spectroscopy (ICP, Perkin-Elmer PLASMA-2000). The products were also characterized by infrared spectroscopy (IR, Perkin-Elmer PE-1600), thermogravimetry, and differential thermal analysis (TG-DTA, Netzsch STA-429).

III. Results

(1) Phase and Grain Size

The analysis results for the chemical composition of the used precursor and the hydrothermal powders synthesized in the reaction medium with different pH values at 200°C for 18 h are shown

I-W. Chen—contributing editor

Manuscript No. 188822. Received January 10, 2000; approved March 13, 2002.
Supported by the National Sciences Foundation of China (NSFC) under Grant No. 59832080.

Table I. Chemical Compositions of the Used Precursor and the Hydrothermal Powders

Sample	Reaction temp and time	pH value of the used medium	Component content (wt%)			
			CeO_2	H_2O	CO_2	SO_3
Precursor			83	12.7	1.5	3.2
Powder 1	200°C, 18 h	12	88.6	6.8	1.4	2.9
Powder 2		7	90.1	5.8	1.1	2.7
Powder 3		2	95.3	4.4	0.2	0.4

in Table I. It can be found that the lower the pH of the reaction medium, the lower the moisture content of the sample, which means that the dewatering of the precursor in the acid medium was more complete than that in the basic medium. The XRD patterns of the samples are shown in Fig. 1. The used precursor and the hydrothermal powders displayed all of the major diffraction peaks of CeO_2 with the fluorite structure.

The relationship between reaction temperature and the grain size of the powders synthesized in the hydrothermal medium with different acidities is shown in Fig. 2. Figure 3 shows the relationship between reaction time and the grain size of the powders synthesized at 200°C.

(2) Morphology

TEM photographs of the used precursor and the powders synthesized at different hydrothermal reaction temperature for 18 h are shown in Fig. 4. Some TEM photographs of the powders synthesized at 200°C for different reaction times are shown in Fig. 5.

In this paper, it is obvious that hydrothermal treatment of $Ce(OH)_4$ is an Ostwald ripening process and the acidity has considerably influenced the hydrothermal treatment process.

(3) IR Spectrograms

IR spectrograms of the used precursor and hydrothermal powders synthesized at 200°C for 18 h in the medium with various acidities are displayed in Fig. 6. It is well known that the broad absorption band located in the area from 3200 to 3600 cm^{-1} approximately corresponds to the O–H stretching vibration, and the one located in the area from 400 to 750 cm^{-1} to the CeO_2 stretching vibration. The absorption peaks at 1600, 1500, or 1340 cm^{-1}, and 1060 cm^{-1} correspond to the H_2O bending vibration, the CO_3^{2-} stretching vibration, and the Ce–OH or SO_4^{2-} stretching vibration, respectively. From Fig. 6, it can be concluded that the crystallization of the powders synthesized in an acidic hydrothermal medium was more complete than others, which agrees with the analysis for the chemical compositions of the samples given in Table I. Figure 6 and Table I show that the hydrothermal treatment processes are associated with SO_4^{2-} and CO_3^{2-}.

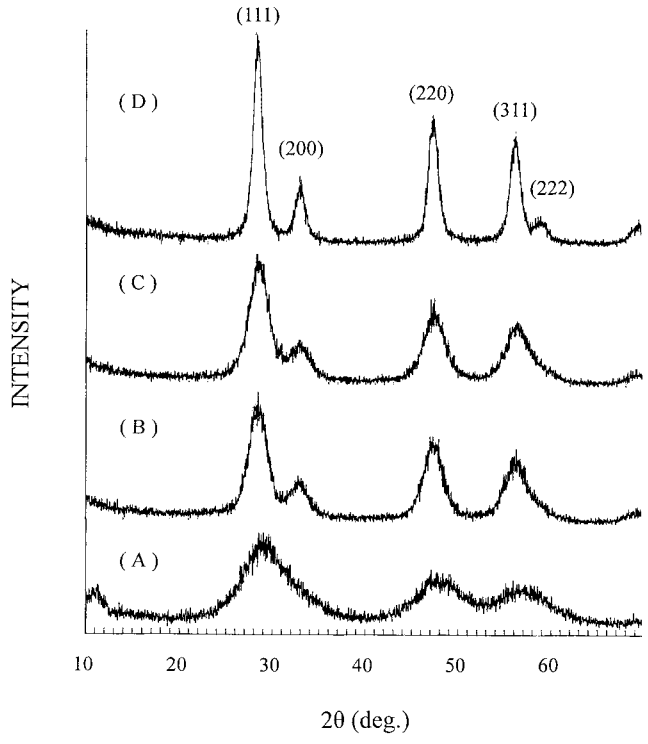

Fig. 1. X-ray diffraction patterns of the used precursor (A) and the hydrothermal powders synthesized at 200°C for 18 h in the reaction medium with a pH of 12 (B), 7 (C), and 2 (D).

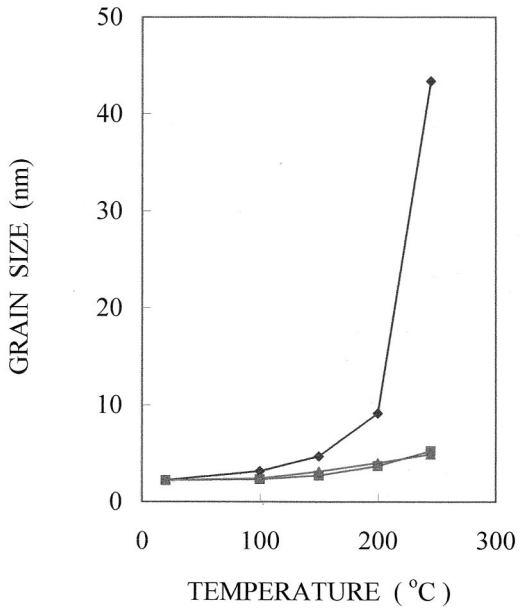

Fig. 2. Relationship between the particle size of the powders and the reaction temperature. The reaction time was fixed at 18 h. (◆) Acidic medium; (■) neutral medium; (▲) basic medium.

(4) TG-DTA Spectrograms

The TG-DTA spectrograms of the used precursor and the hydrothermal powders are shown in Fig. 7. The ascent of the TG curve denotes an increase of sample weight, and it is expressed by positive Δm; and the descent of the TG curve denotes a decrease

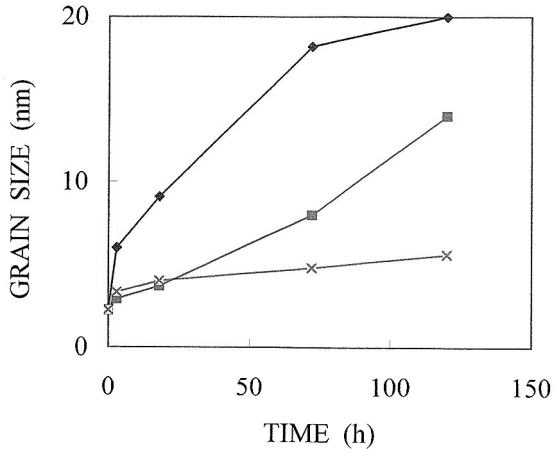

Fig. 3. Relationship between the particle size of the powders and the reaction time. The reaction temperature was fixed at 200°C. (◆) Acidic medium; (■) neutral medium; (×) basic medium.

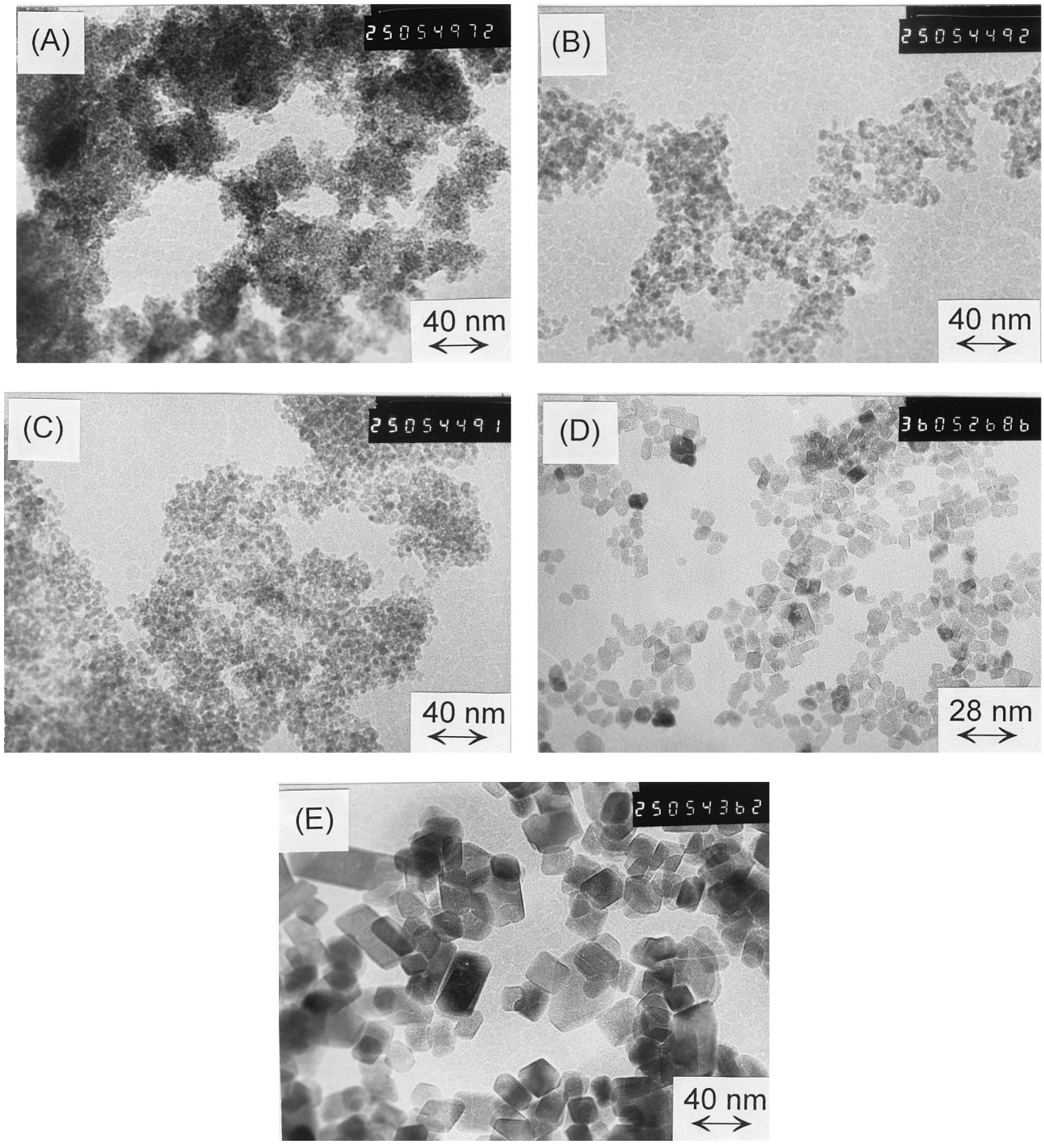

Fig. 4. TEM photographs of the used precursor (A) and the hydrothermal powders synthesized at 245°C in the neutral medium (B) and the basic medium (C), and at 200° (D) and 245°C (E) in the acid medium. The reaction time was fixed at 18 h.

of sample weight, and it is expressed by negative Δm. When the TG curves are out of range of the plotter and are divided into two parts, the total Δm is equal to the algebraic sum of the two parts Δm. Similarly, when the DTA curves are out of range and are divided into two parts, the whole curve may be obtained by joining the two parts after shifting vertically the divided part. The dotted curves indicate a temperature change from room temperature to 1000°C, an ascent of the curve denotes a rise in temperature, and a descent of the curve denotes a fall in temperature. The whole curve may be obtained by joining the divided parts after shifting vertically the divided parts. The endothermic peaks with the temperature below 150°C are related to dehydrating of the examined samples.

IV. Discussion

(1) Formation of CeO_2 Crystallites Synthesized under Hydrothermal Conditions

Because the solubility products[18] of some precipitated substances are bigger (for example, $K_{sp}(AgCl) = 1.8 \times 10^{-10}$ and $K_{sp}(BaSO_4) = 1.1 \times 10^{-10}$, etc), when Ostwald ripening occurs the smaller grains dissolve more quickly, the solute diffuses more slowly, and the larger grains grow more slowly; therefore, it is assumed that the growth kinetics are controlled by diffusion or surface reaction. However, the solubility product[18] of $Ce(OH)_4$ (i.e., $CeO_2 \cdot 2H_2O$) is 2×10^{-48} and is far smaller than for one of those precipitated substances. When Ostwald ripening occurs, the

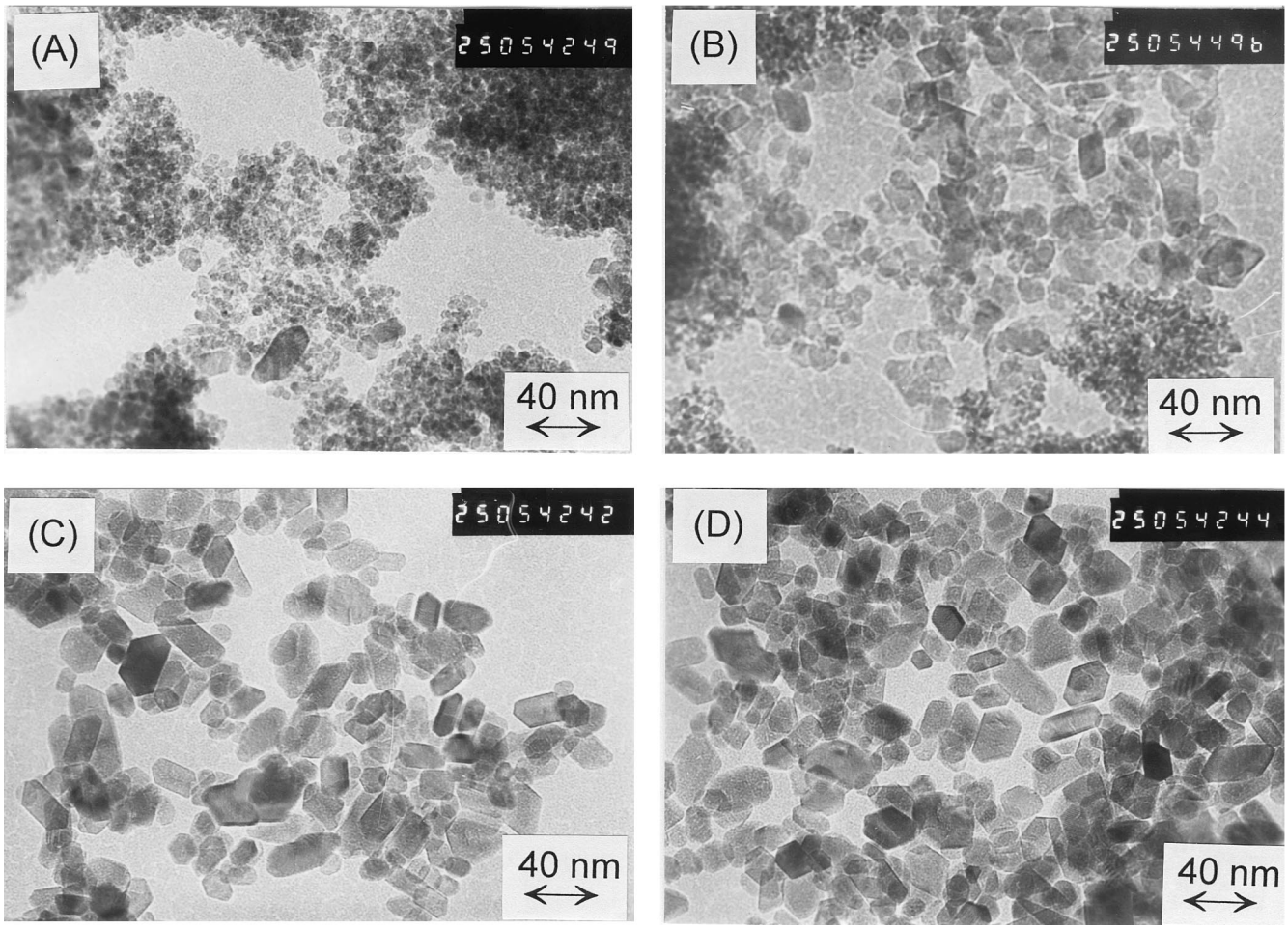

Fig. 5. TEM photographs of the hydrothermal powders synthesized in the neutral medium for 72 (A) and 120 h (B), and in the acidic medium for 72 (C) and 120 h (D). The reaction temperature was fixed at 200°C.

smaller grains dissolve far more slowly, and in addition, grains of precipitated $Ce(OH)_4$ cluster together to form agglomerates, so the solute diffuses more quickly and the larger grains grow more quickly. Therefore, it is assumed that the growth kinetics are controlled by dissolution.

$Ce(OH)_4$ is a basic precipitate, so increasing $[OH^-]$ will lead to an apparent decrease of solubility of $Ce(OH)_4$, and increasing $[H^+]$ will lead to a sizable increase of solubility of $Ce(OH)_4$.

For Ostwald ripening, there is an equilibrium value for grain size r^*. When r is smaller than r^*, smaller grains will dissolve and eventually disappear. When r is larger than r^*, larger grains will grow. The relationship between grain size and solubility may be expressed by the Gibbs–Thomson equation:[19]

$$C(r) = C_\infty \exp(2\gamma V_m/vRTr)$$

where $C(r)$ is the solubility of a grain with radius r, C_∞ is the normal equilibrium solubility of the substance ($r \to \infty$), γ is the interfacial tension, V_m is the molar volume of the solute, v is the number of ions in the formula unit, r is the grain radius, R is the gas constant, and T is the absolute temperature.

According to the maximal growth law of crystal growth,[20] the growth rate of the crystal can be written as

$$R = \beta\sigma \tag{1}$$

where R is the growth rate of the crystal, β is a kinetic coefficient, and σ is the relative supersaturation. It is assumed that the maximal growth law holds true in this paper. σ is defined as

$$\sigma = \exp(\Delta\mu/kT) - 1 \tag{2}$$

where $\Delta\mu$ is the driving force of the crystallization, k is the Boltzmann constant, and T is the absolute temperature. In the solution systems $\Delta\mu$ can be expressed as

$$\Delta\mu = kT \ln C/C_0 \tag{3}$$

where C is the concentration of the supersaturated solution, and C_0 is the concentration of the saturated solution. From Eqs. (1) to (3), the following formula can be obtained:

$$R = \beta(C - C_0)/C_0 \tag{4}$$

This formula shows that, with increasing C, R will increase gradually; and with decreasing C, R will decrease gradually until C is equal to C_0 and a new dissolution–recrystallization equilibrium is established. This can be represented as[21]

$$2CeOH^{3+} = [CeOCe]^{6+} + H_2O \quad (K_5 = 16.5) \tag{5}$$

In this paper, the concentration of the species $CeOH^{3+}$ is taken for the concentration of the solute and is equal to C_∞. In Eq. (4), C is equal to $C(r)$ and C_0 is equal to C^* (the solubility while r is equal to r^*). So Eq. (4) can be represented as

$$R = \beta[C_\infty \exp(2\gamma V_m/vRTr)/C^* - 1]$$

This formula indicates that R is associated with C_∞.

Strictly speaking, the formula of the reactant or product in the hydrothermal medium should be written as $Ce_uO_v(OH)_w(H_2O)_x(SO_4)_y(CO_3)_z$. However, in this paper, the reactants or products are respectively represented as Ce^{4+},

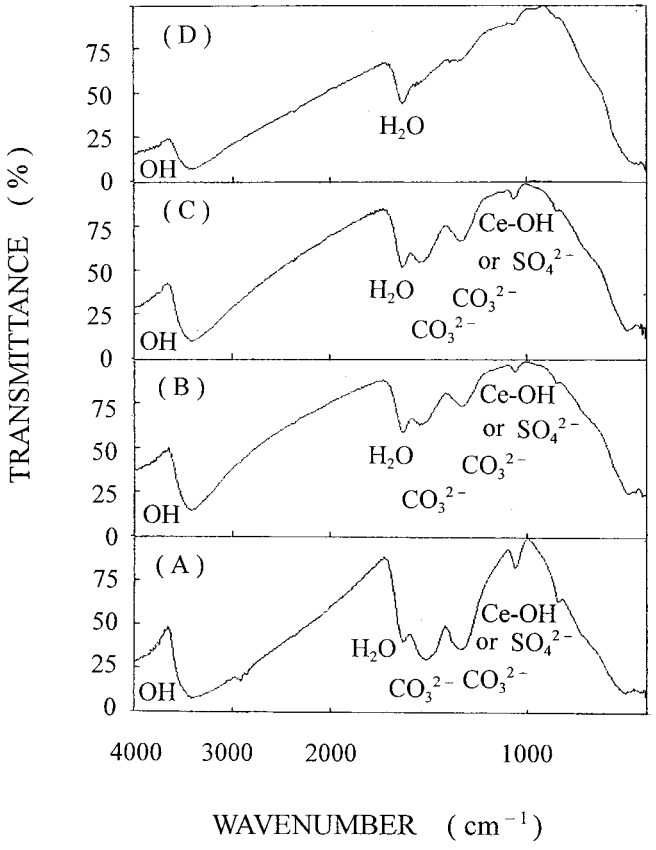

Fig. 6. IR spectra of the used precursor (curve A) and the hydrothermal powders synthesized in the basic medium (curve B), the neutral medium (curve C), and the acidic medium (curve D). The reaction temperature and the time were fixed at 200°C and 18 h.

$CeOH^{3+}$, $CeSO_4^{2+}$, $CeOHCO_3^{+}$, etc., in each chemical equation for simplicity. In this paper, the equilibrium constants at 25°C are applied. The effect of the temperature on the equilibrium constant of the reaction limited only to Eqs. (5) and (8) are discussed; the effect of the temperature on other reactions is not discussed for lack of thermodynamic data. Under certain conditions, all reactions discussed in this paper are reversible.

In $Ce(SO_4)_2$ solution some chemical equilibria are established:[22,21,18]

$$CeSO_4^{2+} + HSO_4^- = Ce(SO_4)_2 + H^+ \quad (K_6 = 200) \tag{6}$$

$$Ce^{4+} + HSO_4^- = CeSO_4^{2+} + H^+ \quad (K_7 = 3500) \tag{7}$$

$$Ce^{4+} + H_2O = CeOH^{3+} + H^+ \quad (K_8 = 5.2) \tag{8}$$

$$H^+ + OH^- = H_2O \quad (K_9 = 10^{14}) \tag{9}$$

When the $Ce(SO_4)_2$ solution was added to the NaOH solution to prepare precursor, the following reactions took place:

$$CeSO_4^{2+} + OH^- + HSO_4^- = Ce(SO_4)_2 + H_2O \quad (K_{10} = 200 \times 10^{14}) \tag{10}$$

$$Ce^{4+} + OH^- + HSO_4^- = CeSO_4^{2+} + H_2O \quad (K_{11} = 3500 \times 10^{14}) \tag{11}$$

$$Ce^{4+} + OH^- = CeOH^{3+} \quad (K_{12} = 5.2 \times 10^{14}) \tag{12}$$

Equations (10), (11), and (12) can be obtained respectively from Eqs. (6), (7), and (8) combined with Eq. (9). When the concentration of $CeOH^{3+}$ increases, other reactions take place:

$$CeOH^{3+} + HCO_3^- + OH^- = CeOHCO_3^+ + H_2O \quad (K_{13} = 9.02 \times 10^4)$$
$$\hookrightarrow CeOCO_3 + H^+ \tag{13}$$

$$2CeOH^{3+} = [CeOCe]^{6+} + H_2O \quad (K_5 = 16.5) \tag{5}$$

Under certain conditions, the following reactions may take place:[18]

$$HCO_3^- = H^+ + CO_3^{2-} \quad (K_{14} = 4.7 \times 10^{-11}) \tag{14}$$

$$CeOH^{3+} + H^+ = Ce^{4+} + H_2O \quad (K_{15} = 0.192) \tag{15}$$

Reaction (15) is the backward reaction of reaction (8). In Ref. 23 the following reaction is proposed:

$$Ce^{4+} + NO_3^- + H_2O = Ce(OH)(NO_3)^{2+} + H^+ \quad (K_{16} = 10^2) \tag{16}$$

In Refs. 24 and 25, some evidence otherwise shows that $Ce(OH)(CO_3)$ is stable, so it is suggested that the following reaction can occur:

$$Ce^{4+} + CO_3^{2-} + H_2O = CeOHCO_3^+ + H^+ \quad (K_{17} = 10^2)$$
$$\hookrightarrow CeOCO_3 + H^+ \tag{17}$$

In fact, because CO_3^{2-} has two negative charges and will produce greater crystal lattice energy than NO_3^-, we think that a Ce^{4+} complex with CO_3^{2-} is more stable than a Ce^{4+} complex with NO_3^-. Moreover, it appears that $CeOCO_3$ can be stable as $Ce(OH)(CO_3)$. By combining Eqs. (9), (14), (15), and (17), Eq. (13) can be obtained, as shown above.

Hydrolysis and dimerization reactions took place successively (Eqs. (8) and (5)), leading to the formation of CeO_2 grains. Because the concentration of $CeOH^{3+}$ increased rapidly, a great number of CeO_2 nuclei formed in a very short time. Equations (10), (11), and (13) show that in basic solution $CeSO_4^{2+}$, $Ce(SO_4)_2$, and $CeOHCO_3^+$ are quite stable, and it is quite difficult for a Ce^{4+} complex with SO_4^{2-} or CO_3^{2-} to be resolved, so that it is difficult for the nuclei which combine with SO_4^{2-} or CO_3^{2-} on the surface to grow further.

Under certain conditions, the following equilibria can be established:

$$Ce(SO_4)_2 + H^+ = CeSO_4^{2+} + HSO_4^- \quad (K_{18} = 5 \times 10^{-3}) \tag{18}$$

$$CeSO_4^{2+} + H^+ = Ce^{4+} + HSO_4^- \quad (K_{19} = 2.86 \times 10^{-4}) \tag{19}$$

$$CeOHCO_3^+ + H^+ = Ce^{4+} + CO_3^{2+} + H_2O \quad (K_{20} = 10^{-2}) \tag{20}$$

Reactions (18), (19), and (20) are the backward reactions of Eqs. (6), (7), and (17), respectively. With the sum of reactions (18), (19), and (8), an overall reaction can be obtained:

$$Ce(SO_4)_2 + H^+ + H_2O = CeOH^{3+} + 2HSO_4^- \quad (K_{21} = 7.42 \times 10^{-6}) \tag{21}$$

With the sum of reactions (8) and (20) and the backward reaction of Eq. (14), an overall reaction can be obtained:

$$CeOHCO_3^+ + H^+ = CeOH^{3+} + HCO_3^- \quad (K_{22} = 1.1 \times 10^9) \tag{22}$$

Under hydrothermal conditions, with increasing temperature the equilibrium of reaction (8) shifts toward the right,[21] so that the concentration of the hydrogen ion is increased. This leads to a transformation such that the equilibria of reactions (21) and (22)

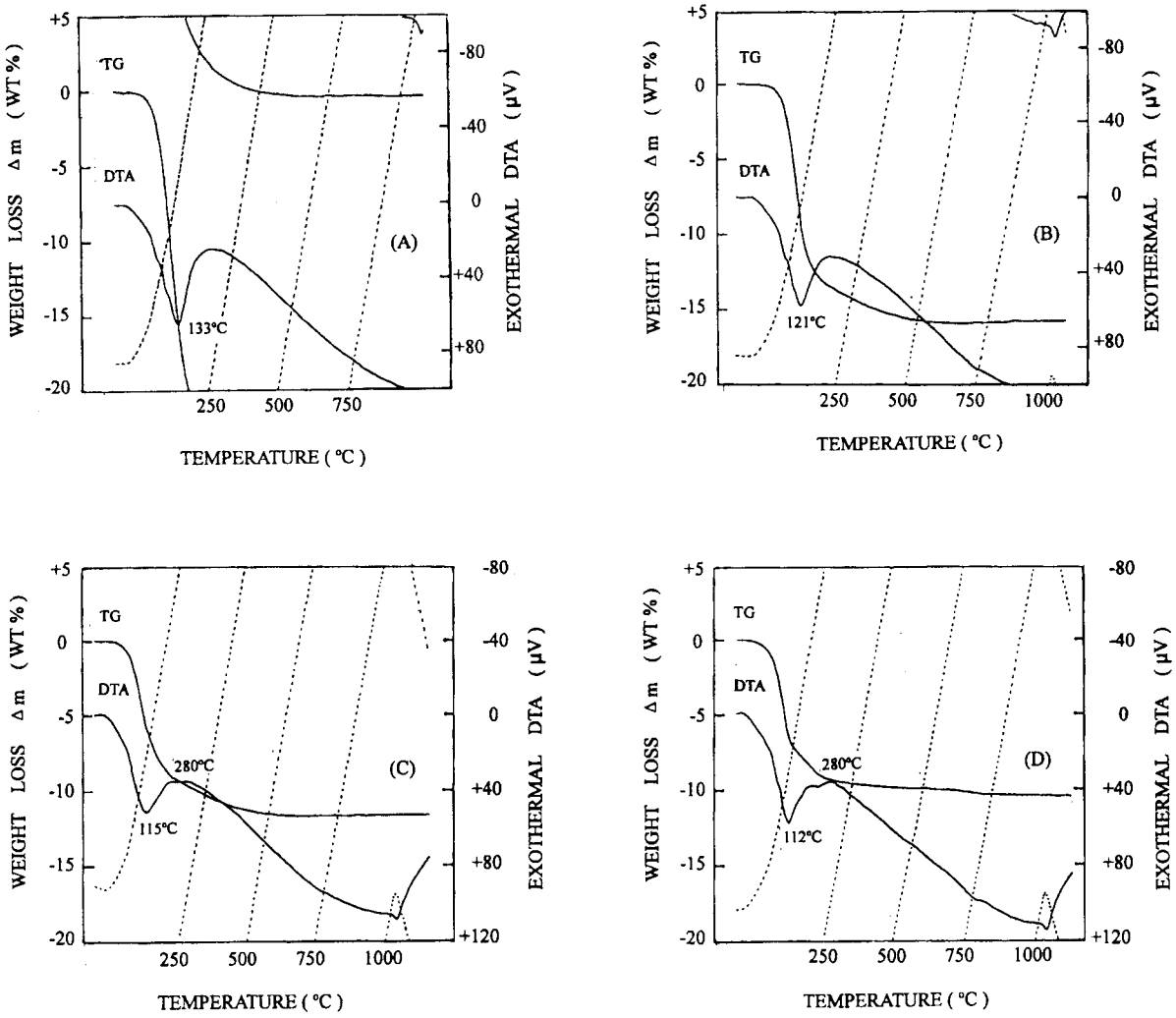

Fig. 7. TG-DTA spectra of the used precursor (A) and the hydrothermal powders synthesized in the basic medium (B), the neutral medium (C), and the acidic medium (D). The reaction temperature and the time were fixed at 200°C and 18 h.

shift toward the right and the concentrations of $Ce(SO_4)_2$ or $CeOHCO_3^+$ decrease while the concentration of $CeOH^{3+}$ increases, so the equilibrium of dissolution–recrystallization shifts toward crystallization as in reaction (5).

With the combination of reactions (5) and (8), the following equation can be obtained:

$$2Ce^{4+} + H_2O = [CeOCe]^{6+} + 2H^+ \quad (K_{23} = 4.5 \times 10^2) \tag{23}$$

Reaction (23) shows that with an increase in the concentration of hydrogen ion the equilibrium of reaction (23) moves to the left and the movement facilitates dissolution of the precursor. The key step for the hydrothermal synthesis of CeO_2 powders is the dissolution of the precursor.

When the hydrothermal medium was adjusted to basicity, with an increasing temperature the following reactions occurred until equilibrium was reached:

$$Ce(SO_4)_2 + 2H_2O = 2HSO_4^- + OH^- + CeOH^{3+} \quad (K_{24} = 7.42 \times 10^{-20}) \tag{24}$$

$$CeOHCO_3^+ + H_2O = HCO_3^- + OH^- + CeOH^{3+} \quad (K_{25} = 1.1 \times 10^{-5}) \tag{25}$$

Reaction (24) can be obtained by combining the backward reactions of Eqs. (10) and (11) and reaction (12). Reaction (25) is the backward reaction of Eq. (13). Because K_{24} and K_{25} were quite small and the concentration of the hydroxide ion was high, the dissolution of the grains of the precursor was very limited and the amount of SO_4^{2-} and CO_3^{2-}, which transferred from solid-phase grains to liquid-phase medium, was very low, so the SO_4^{2-} and CO_3^{2-} content in the solid phase was greater. Because Ostwald ripening proceeded to a very slight extent, the size of the grains increased only slightly.

When the hydrothermal medium was adjusted to neutrality, the equilibria of reactions (24) and (25) shifted toward the right because the concentration of the hydroxide ion was decreased, and the concentration of $CeOH^{3+}$, HCO_3^-, and HSO_4^- were increased. Therefore, the CO_2 and SO_3 contents of the powder obtained in neutral hydrothermal medium were lower. It took a longer time to grow grains and reach dissolution–recrystallization equilibrium for smaller K_{24} and K_{25}.

When the hydrothermal medium was adjusted to acidity, the following reactions took place:

$$Ce(SO_4)_2 + H^+ + H_2O = CeOH^{3+} + 2HSO_4^- \quad (K_{21} = 7.42 \times 10^{-6}) \tag{21}$$

$$CeOHCO_3^+ + H^+ = CeOH^{3+} + HCO_3^- \quad (K_{22} = 1.1 \times 10^9) \tag{22}$$

Because K_{21} and K_{22} were respectively greater than K_{24} and K_{25} and the concentration of the hydrogen ion was increased greatly, the

equilibria of reactions (21) and (22) lay to the right. With the dissolution of smaller grains, bigger grains grew further until a new dissolution–recrystallization was reached. Because the smaller grains were dissolved in great quantities, the SO_4^{2-} and CO_3^{2-} in the smaller grains were transferred to the liquid medium and the SO_4^{2-} and CO_3^{2-} contents in the solid grains which had grown were decreased greatly. With smaller grains dissolving, Ostwald ripening proceeds at a more rapid rate and the larger grains grow in a shorter time.

In fact, under hydrothermal conditions the CeO_2 grains were formed through a series of hydrolysis and polymerism. However, a dimerism reaction is applied for simplicity when the hydrothermal reaction mechanisms are discussed. Although the equilibrium constant of the dimerism reaction is only 16.5, the equilibrium constant of the overall reaction has a very big value, if a series of the hydrolysis and polymerism reactions occurring successively are combined. According to the fact that the solubility product[18] of $Ce(OH)_4$ (i.e., $CeO_2 \cdot 2H_2O$) is equal to 2×10^{-48}, it can also be thought that CeO_2 in aqueous solution is very stable and the equilibrium constant of polymerism is quite large. Therefore, with combination of reaction (21) and the polymerism reaction, the equilibrium constant of the overall reaction is quite large, and the equilibrium is displaced so that the reactant $Ce(SO_4)_2$ decreases and the product CeO_2 increases even though the equilibrium constant of reaction (21) is smaller.

(2) Formation and the Elimination of Agglomeration

It is known that agglomeration is usually harmful to applications of materials and should be avoided. Agglomeration occurs because of electrostatic forces, van der Waals forces, capillary forces, etc. However, some forces can be eliminated in nanocrystalline CeO_2 powders prepared by hydrothermal methods, so that agglomeration can be greatly reduced. The equilibrium constants of reactions (10) to (13) show that $Ce(SO_4)_2$, $CeSO_4^{2+}$, $CeOH^{3+}$, and $CeOHCO_3^+$ are quite stable in basic solution. Usually, grain surfaces absorb water molecules, so that hydrogen bonds can be formed between two approaching grains as follows:

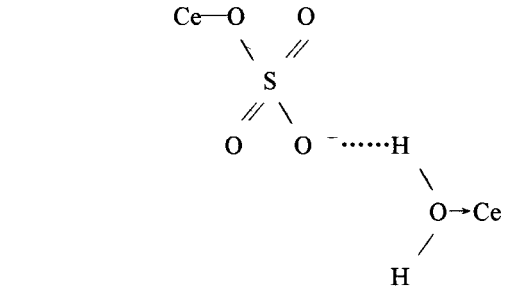

and

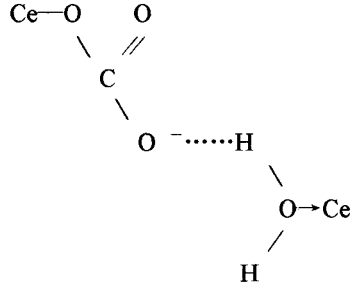

Therefore, hydrogen bonding can lead to vigorous agglomeration of grains. Agglomeration will be increased in grains obtained in basic medium for SO_4^{2-} and CO_3^{2-}, and agglomeration will be reduced greatly in grains obtained in acidic medium for the removal of SO_4^{2-} and CO_3^{2-}.

IV. Conclusions

(1) Well-crystallized cerium(IV) oxide powders with nanosizes without agglomeration were synthesized under hydrothermal conditions in an acidic medium, if the cerium hydroxide gel produced by mixing $Ce(SO_4)_2$ and NaOH solutions was used as the precursor.

(2) The synthesis of the powders under hydrothermal conditions is thought to be Ostwald ripening. The key step in the process is the dissolution of the precursor, which includes the resolution of SO_4^{2-} or CO_3^{2-} combined with a Ce^{4+} complex, and the pH of the hydrothermal medium has an important effect on the dissolution of the precursor. In an acidic medium, with the dissolution of the precursor, the grain growth is more rapid; and in a basic medium, the grain growth is slower.

(3) In this paper, it is thought that agglomeration may be caused by the combination of SO_4^{2-} or CO_3^{2-} with Ce^{4+} on the surfaces of two approaching grains and the hydrogen bonding between two approaching grains. In an acidic hydrothermal medium, with dissolution of the precursor, the ions SO_4^{2-}, CO_3^{2-}, and OH^- on the surfaces of the grains are replaced by water molecules; therefore, the combination of SO_4^{2-} or CO_3^{2-} with Ce^{4+} and hydrogen bonding decrease greatly, so that the agglomeration is reduced greatly.

References

[1]C. Tian and S. Chan, "Microstructural Correlation with Electrical Properties for Doped CeO_2 Thin Films"; pp. 279–84 in Materials Research Society Symposium Proceedings, Vol. 500, *Electrically Based Microstructural Characterization II*. Edited by R. A. Gerhardt, M. A. Alim, and S. R. Taylor. Materials Research Society, Pittsburgh, PA, 1998.

[2]T. Mon and H. Yamamura, "Preparation of an Alkali-Element or Alkali-Earth-Element-Doped CeO_2–Sm_2O_3 System and Its Operation Properties as the Electrolyte in Planar Solid Oxide Fuel Cell," *J. Mater. Synth. Process.*, **6** [3] 175–79 (1998).

[3]J. I. Hamagami, Y. Inda, T. Umegaki, and K. Yamashita, "High Temperature pH Sensing and O^{2-} Conduction Properties of Electrophoretically Fabricated Ceria Composites," *Solid State Ionics*, **113–115**, 235–39 (1998).

[4]F. Fajardie, J. F. Tempere, J. M. Manoli, O. Touret, G. Blanchard, and G. Djega-Mariadassou, "Activity of RH^{X+} Species in CO Oxidation and NO Reduction in a CO/NO/O_2 Stiochiometric Mixture over a RH/CeO_2–ZrO_2 Catalyst," *J. Catal.*, **179** [2] 469–76 (1998).

[5]T. Chafik, O. Dulaurent, J. L. Gass, and D. Bianchi, "Heat of Adsorption of Carbon Monoxide on a Pt/Rh/CeO_2/Al_2O_3 Three-Way Catalyst Using *In Situ* Infrared Spectroscopy at High Temperatures," *J. Catal.*, **179** [2] 503–14 (1998).

[6]E. Bekyarova, P. Fornasiero, J. Kaspar, and M. Graziani, "CO Oxidation on Pd/CeO_2–ZrO_2 Catalysts," *Catal. Today*, **45** [1–4] 179–83 (1998).

[7]Y. Hakuta, S. Onai, S. Terayama, T. Adschiri, and K. Arai, "Production of Ultra-fine Ceria Particles by Hydrothermal Synthesis under Supercritical Conditions," *J. Mater. Sci. Lett.*, **17** [14] 1211–13 (1998).

[8]S. Dikmen, P. Shuk, and M. Greenblatt, "Hydrothermal Synthesis and Properties of $Ce_{1-x}Bi_xO_{2-\delta}$ Solid Solutions," *Solid State Ionics*, **112** [3–4] 299–307 (1998).

[9]Y. C. Zhou and M. N. Rahamain, "Hydrothermal Synthesis and Sintering of Ultrafine CeO_2 Powders," *J. Mater. Res.*, **8** [7] 1680–86 (1993).

[10]E. Tani, M. Yoshimura, and S. Somiya, "Crystallization and Crystal Growth of CeO_2 under Hydrothermal Conditions," *J. Mater. Sci. Lett.*, **1**, 461–62 (1982).

[11]M. Hirano and E. Kato, "Hydrothermal Synthesis of Nanocrystalline Cerium(IV) Oxide Powders," *J. Am. Ceram. Soc.*, **82** [3] 786–88 (1999).

[12]E. Matijevic and W. P. Hsu, "Preparation and Properties of Monodispersed Colloidal Particles of Lanthanide Compounds: I, Gadolinium, Europium, Terbium, Samarium, and Cerium(III)," *J. Colloid Interface Sci.*, **118**, 506–23 (1987).

[13]X. Chu, W. Chung, and L. D. Schmidt, "Sintering of Sol-Gel-Prepared Submicrometer Particles Studied by Transmission Electron Microscopy," *J. Am. Ceram. Soc.*, **76** [8] 2115–18 (1993).

[14]P. L. Chen and I-W. Chen, "Reactive Cerium(IV) Oxide Powders by the Homogeneous Precipitation Method," *J. Am. Ceram. Soc.*, **76** [6] 1577–83 (1993).

[15]T. J. Kirk and J. Winnick, "A Hydrogen Sulfide Solide-Oxide Fuel Cell Using Ceria-Based Electrolytes," *J. Electrochem. Soc.*, **140**, 3494–96 (1993).

[16]K. Higashi, K. Sonoda, and H. Ono, S. Sameshima, and Y. Hirata, "Characterization of Rare-Earth-Doped Ceria Powders Derived from Oxalate Coprecipitate," *Key Eng. Mater.*, **159–160**, 25–30 (1999).

[17]A. Suda, H. Sobukawa, T. Suzuki, T. Kandori, Y. Ukyo, and M. Sugiura, "Synthesis of Ceria–Zirconia Solid Solution and Its Performance as Catalytic Promoter," (in Jpn.), *Toyota chu-ou Kenkyusho R&D Rebyu*, **33** [3] 3–12 (1998).

[18]J. A. Dean (ed.), *Lange's Handbook of Chemistry*, 13th Ed. McGraw-Hill, New York, 1985.

[19]J. W. Mullin, "Ripening"; p. 288 in *Crystallization*, 3rd Ed. Butterworth-Heinemann, Oxford, England, 1997.

[20]J. P. van der Eerden, "Crystal Growth Mechanisms", p. 315 in *Handbook of Crystal Growth*. Edited by D. T. J. Hurle. Elsevier Science Publishers, Amsterdam, Netherlands, 1993.

[21]T. J. Hardwick and E. Robertson, "Ionic Species in Ceric Perchlorate Solution," *Can. J. Chem.*, **29**, 818–27 (1951).

[22]Reference 21, pp. 828–37.

[23]E. Wadsworth, F. R. Duke, and C. A. Goetz, "Present Status of Cerium(IV)–Cerium(III) Potentials," *Anal. Chem.*, **29** [12] 1824–25 (1957).

[24]E. Matijevic and W. P. Hsu, "Preparation and Properties of Monodispersed Colloidal Particles of Lanthanide Compounds," *J. Colloid Interface Sci.*, **118** [2] 506–23 (1987).

[25]M. Hirano and E. Kato, "Hydrothermal Synthesis of Two Types of Cerium Carbonate Particles," *J. Mater. Sci. Lett.*, **18**, 403–405 (1999). □